Volume 8, Issue 3, 2018, 3232 - 3236 ISSN 2069-5837

Biointerface Research in Applied Chemistry

www.BiointerfaceResearch.com

Original Research Article Open Access Journal

Received: 05.05.2018 / Revised: 30.05.2018 / Accepted: 10.06.2018 / Published on-line: 15.06.2018

Dynamic analysis of bovine hydroxyapatite/$CaTiO_3$ bioceramics

Suat Ozturk [1], Mehmet Yetmez [2,*]

[1]DERAC, Bulent Ecevit University, Zonguldak, Turkey

[2]Department of Mechanical Engineering, Bulent Ecevit University, Zonguldak, Turkey

*corresponding author e-mail address: **yetmez@beun.edu.tr**

ABSTRACT

In this study, modal analysis and vibro-acoustic investigation are considered to determine dynamic characteristics of bovine hydroxyapatite/calcium titanate bioceramics. Results show that first natural frequencies increase with increasing sintering temperature for all groups. The addition of calcium titanate to bovine hydroxyapatite causes the natural frequency to ascend. Similarly, damping ratios for all groups go up with increasing sintering temperature and calcium titanate addition to bovine hydroxyapatite raises damping ratios for vibration. The addition of calcium titanate to bovine hydroxyapatite significantly raises sound damping capability and damping slightly increases with raising sintering temperature.

Keywords: *Bovine hydroxyapatite; Calcium titanate; Bioceramics; Natural frequency; Damping; Vibro-acoustic.*

1. INTRODUCTION

Biomaterials hold a very important place in human's health. Crucial one of these materials is hydroxyapatite and its derivatives as bio-active ceramics used frequently in operative treatments for bone replacement, regeneration and repairement [1-8]. Hydroxyapatite that is the main inorganic component of bones has excellent osteoconductivity, biocompatibility, and bioactive properties, but poor brittleness, fracture toughness, corrosion resistance and electrical conductivity [9-16]. To improve its poor properties, hydroxyapatite based ceramics are mostly produced by sintering at a proper temperature and mixing its powders with other material powders as Ag, Ti, Ce, Zn, MgO, TiO_2, Al_2O_3, $BaTiO_3$ etc [17-24]. Hydroxyapatite produced from bovines is more economic, biocompatible and eco-friend than synthetic one [25].

Calcium titanate ($CaTiO_3$) is one of outstanding materials that has been recently begun to be used in the biomedical area. It is proved that $CaTiO_3$ protects hydroxyapatite not to dissolve in acidic tissue environment, induces apatites to growth, helps osteoblast cells to fasten better to hydroxyapatite and doesn't show any negative reaction in body tissue. Moreover, hydroxyapatite-$CaTiO_3$ composites have a good biocompability, bioactivity and mechanical behavior [26-33].

Ceramics are currently also used in electrical circuit elements, panels of aerospace and marine vehicles. Therefore, natural frequency, damping of vibration and sound, sound transmission and sound caused by vibration become a serious problem to be taken into consideration in all systems [34, 35]. Although there are many studies about hydroxyapatite and hydroxyapatite-$CaTiO_3$ bio-composites to determine and improve physical and mechanical properties, vibration and vibro-acoustic studies for hydroxyapatite-$CaTiO_3$ ceramics are not able to see in the literature.

The main aim of this study is to determine free vibration and vibro-acoustic characteristics of bovine hydroxyapatite (BHA)/$CaTiO_3$ ceramics by taking experimental and numerical modal analysis and experimental vibro-acoustic analysis into account.

2. EXPERIMENTAL SECTION

Generally, the appropriate sintering temperature interval for ceramics is known to be between 1100 and 1200 ^oC because of poorly changing of physical and mechanical properties from the literature. In this study, three test groups are considered: BHA (100 wt. %BHA), 5BHA (95 wt.% BHA and 5 wt.% $CaTiO_3$) and 10BHA (90 wt.% BHA and 10 wt.% $CaTiO_3$) in the range of sintering temperature of 1000-1300 ^oC. Test samples produced according to the British Standard BS 7253 are approximately 10 mm in diameter and 12 mm in height [32].

In the first part, experimental and numerical modal analysis is performed. For the experimental investigation, vibration tests are realized exciting the ceramic specimens by an impulse hammer with a force transducer (Model No: 5800B2, Dytran Instruments, Inc., USA) and collecting the responses by an accelerometer (Model No: 3093B, Dytran Instruments, Inc., USA) in contact to the top surface of a specimen. All modal tests are under clamped-clamped boundary condition (see Figure 1). The tests are completed by using a data acquisition system SoMatTM e-DAQ-lite with Test Control Environment software, nCode GlypWorks (HBM Inc.,USA).

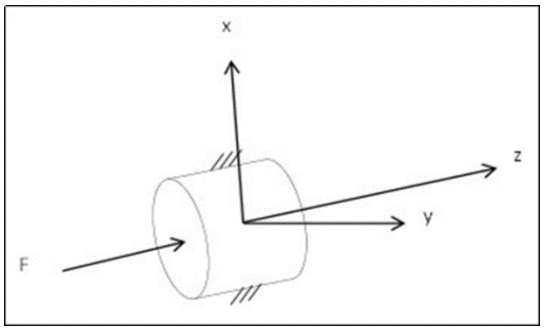

Figure 1. Schematic represantation of cylindric composite sample for the vibration experiment.

In modal tests, the samples are vibrated to breadth in direction Z and lengthy in direction X and Y hammer impacts at

the front face of samples in direction Z. Vibration responds in X, Y, and Z directions collected by a 3-axis accelerometer at the back surface of samples are used to calculate natural frequencies of samples.

The numerical investigation of BHA/$CaTiO_3$ composites is realized by general purpose finite element code ANSYS. The mesh of the model includes 472564 nodes and 113883 elements. The element type of the model is SOLID186. Numerical analysis is carried out by using the average values of mechanical properties of the groups with different sintering temperature as given in Table 1.

Table 1. The average values of mechanical properties of BHA, 5BHA and 10BHA with different sintering temperature [32].

Group	T (^{o}C)	ρ (g/cm^3)	E (GPa)	ν
BHA	1000	1.96	31.1	0.27
BHA	1100	2.13	30.1	0.27
BHA	1200	2.63	96.4	0.27
BHA	1300	2.85	121.8	0.27
5BHA	1000	1.98	24.9	0.27
5BHA	1100	2.13	30.6	0.27
5BHA	1200	2.65	92.9	0.27
5BHA	1300	2.88	107.2	0.27
10BHA	1000	2.02	33.8	0.27
10BHA	1100	2.16	31.9	0.27
10BHA	1200	2.67	85.6	0.27
10BHA	1300	2.92	97.3	0.27

The FE model of the sample created in ANSYS DesignModeller is illusturated in Figure 2.

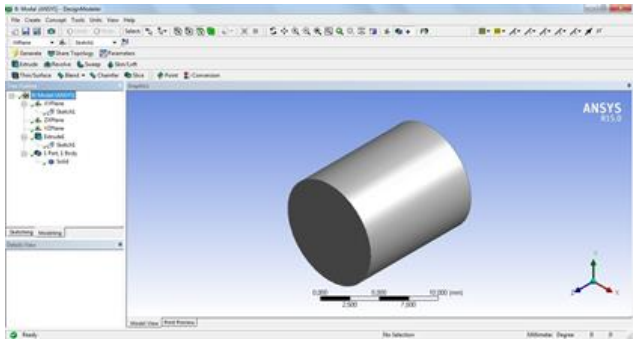

Figure 2. The FE model of the sample in ANSYS.

In the second part, the experimental vibro-acoustic analysis is carried out in a soundproof acoustic demonstrator designed in the inner dimensions of 395 x 205 x 185 mm^3. The sound waves are permanently created by a harmonic excitation source of ±0.5 N and 0-30 Hz fixed very close to the front surface of horizontal cylindrical samples and waves passing through the inside of ceramic samples located tightly in a cylindrically carved wooden base (50x50x12 mm) are collected by ½" free-field microphone set (Type 46AE, G.R.A.S., Denmark) fixed at the distance of 20 mm to the back surface of samples. The test configuration is shown in Figure 3. The vibro-acoustic measurements are conducted via SoMatTM e-DAQ-lite data acquisition system and nCode GlypWorks software (HBM Inc., USA).

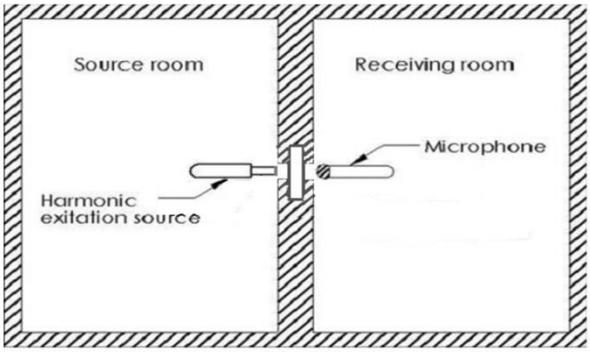

Figure 3. Schematic representation of the vibro-acoustic test setup.

3. RESULTS AND DISCUSSION

3.1. Modal Analysis.

Experimental and numerical results of the first natural frequencies of BHA and BHA/$CaTiO_3$ ceramics are given in Figure 4-6. The first natural frequencies increase with rising sintering temperature. The highest frequency belongs to 10BHA followed by 5BHA and BHA samples in decreasing order. The addition of $CaTiO_3$ to BHA causes the natural frequency to ascend. Comparing the results of modal analyses and experiments, the average percentage deviation of the first natural frequencies for BHA/$CaTiO_3$ ceramics is approximately found 12.8% after adding or subtracting standard deviation values from test results and it is thought to be in reasonable limits for a solid model.

As a result, natural frequencies are very crucial for all systems under repetitive agitating forces. An excitation around 10% of natural frequency creates resonance risk at a system and causes sound augmentation as well.

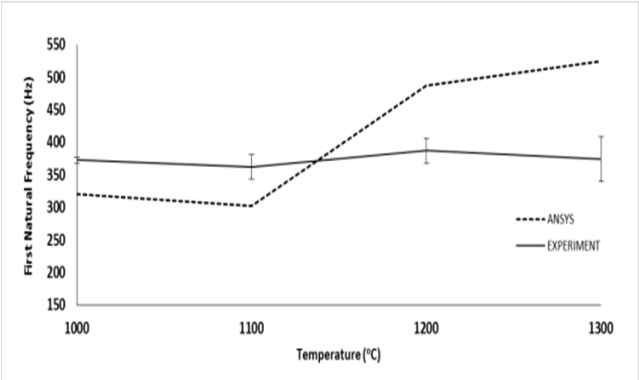

Figure 4. Experimental and numerical comparison of the first natural frequency for BHA.

The first damping ratios obtained from vibration and vibro-acoustic tests are calculated from frequency response function (FRF) diagrams by equation 1. A sample FRF diagram is given in Figure 7.

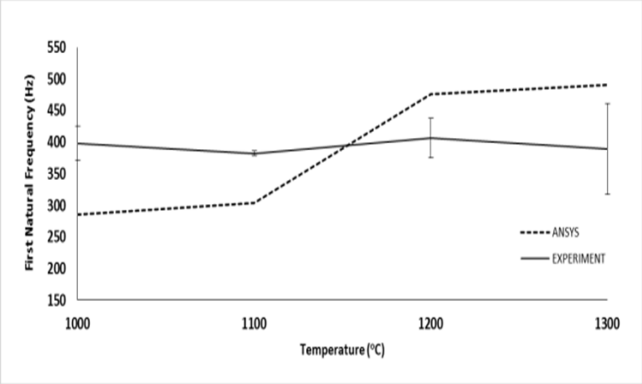

Figure 5. Experimental and numerical comparison of the first natural frequency for 5BHA.

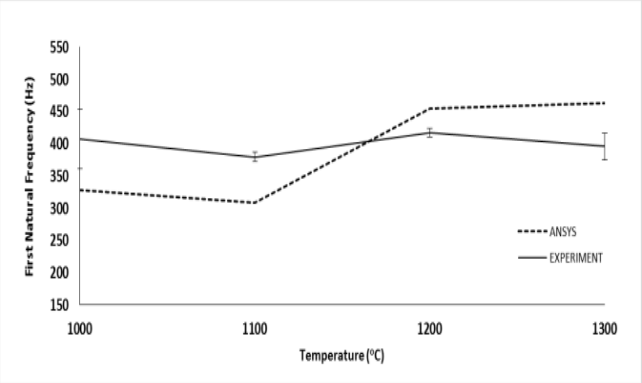

Figure 6. Experimental and numerical comparison of the first natural frequency for 10BHA.

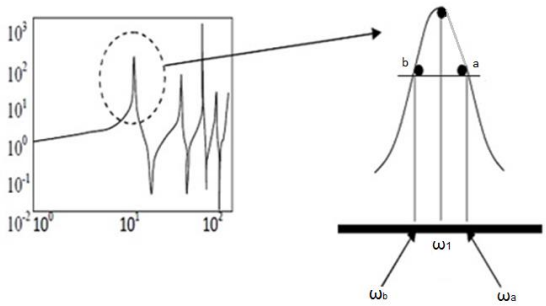

Figure 7. A sample for frequency response function (FRF) diagram [36].

$$\zeta = \frac{\omega_a - \omega_b}{2\omega_1} \qquad (1)$$

The ranking of damping ratios from the highest to the lowest is in the order of 10BHA, 5BHA, and BHA, Figure 8. There is a reduction 10BHA after 1200 ^{o}C. The damping ratios for all test groups go up with increasing sintering temperature and $CaTiO_3$ addition to BHA raises damping ratios.

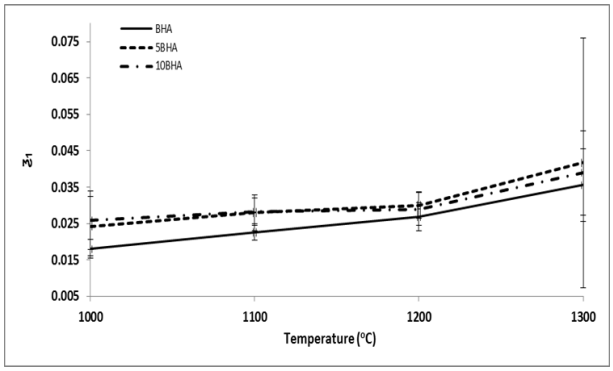

Figure 8. Variation of first damping ratio with sintering temperature for all three groups.

3.2. Vibro-acoustic Analysis

In the result of vibro-acoustic tests, the ranking for natural frequency is at the order of 5BHA, BHA, and 10BHA from the highest to the lowest and close to each other, Figure 9. Increasing sintering temperature barely reduces natural frequencies for all samples. It is seen that there is a difference between the measured values and the orderings of natural frequencies in the results of vibration and vibro-acoustic tests. The reason is that sound waves coming from a harmanic source create low vibration at ceramic samples with a small force (±0.5 N) and continuous. The force applied with hammer impacts in vibration tests is around 8 N and discontinuous.

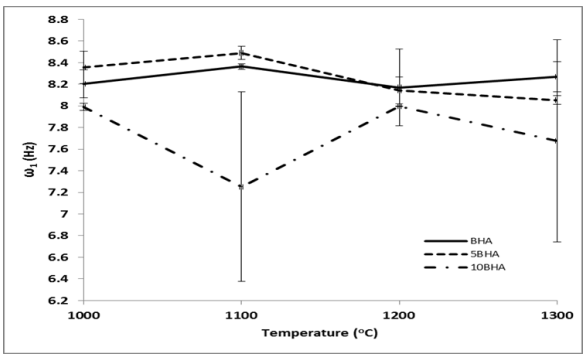

Figure 9. Vibro-acoustic variation of first natural frequency with sintering temperatute for all three groups.

Vibro-acoustic tests are especially important in determining the sound damping property of materials. 10BHA has the highest sound damping values and is followed by 5BHA and BHA ceramics, Figure 10. The addition of $CaTiO_3$ to BHA significantly raises sound damping capability. Damping slightly increases with raising sintering temperature. According to the frequency response model, the vibration is an input-output relation. Output vibration is a multiplication of applied force and frequency response function. So, frequency response function H(f) gives some idea about vibration. The ordering of frequency response function is 10BHA, 5BHA, and BHA from the highest to the lowest, Figure 11. Function values slighly rise with increasing sintering temperature for all samples.

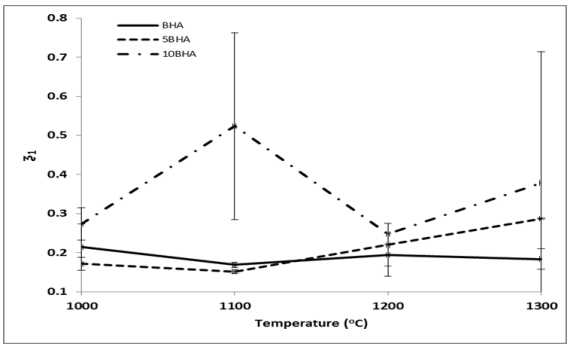

Figure 10. Vibro-acoustic variation of first damping ratio with sintering temperature for all three groups.

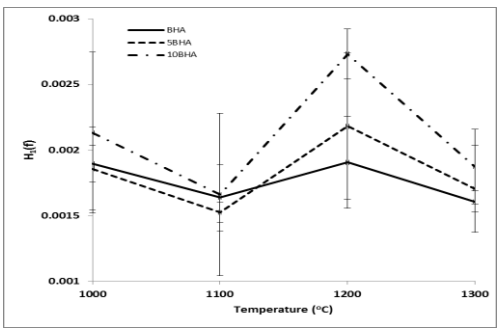

Figure 11. Vibro-acoustic variation of first frequency response function with sintering temperature for all three groups.

4. CONCLUSIONS

According to the results of experimental and numerical modal analyzes, the first natural frequencies increase with rising sintering temperature. The highest frequency belongs to 10BHA ceramics. The addition of $CaTiO_3$ to BHA causes the natural frequency to ascend. The average percentage deviation of the first natural frequencies of BHA/$CaTiO_3$ ceramics is approximately found 12.8% between modal analyses and test results. The ranking of damping ratios from the highest to the lowest is in the order of 10BHA, 5BHA, and BHA. The damping ratios for all test groups go up with increasing sintering temperature and $CaTiO_3$ addition to BHA raises damping ratios.

Vibro-acoustic test results indicate that the ranking for natural frequency is at the order of 5BHA, BHA, and 10BHA from the highest to the lowest and close to each other. Increasing sintering temperature barely reduces natural frequencies for all samples. 10BHA has the highest sound damping values and is followed by 5BHA and BHA ceramics. The addition of $CaTiO_3$ to BHA significantly raises sound damping capability. Damping slightly increases with raising sintering temperature. The ordering of frequency response function is 10BHA, 5BHA, and BHA from the highest to the lowest.

5. REFERENCES

[1] Aminzare M., Eskandari E., Baroonian M. H., Berenov A., Razavi Hesabi Z., Taheri M., Sadrnezhaad S. K., Hydroxyapatite nanocomposites: synthesis, sintering and mechanical properties, *Ceram Int*, 39, 3, 2197-2206, **2013**.

[2] Ooi C. Y., Hamdi M., Ramesh S., Properties of hydroxyapatite produced by annealing of bovine bone, *Ceram Int*, 33, 7, 1171-1177, **2007**.

[3] Niakan A., Ramesh S, Ganesan P, Tan CY, Purbolaksono J, Chadran H, Ramesh S, Teng W. D., Sintering behaviour of natural porous hydroxyapatite derived from bovine bone, *Ceram Int*, 41, 2, 3024-3029, **2015**.

[4] Han S. X., Ning Z. W., Chen K., Zeng J., Preparation and tribological properties of Fe-hydroxyapatite bioceramics, *Biosurface and Biotribology*, 3, 75-81, **2017**.

[5] Kolmas J., Krukowski S., Laskus A., Jurkitewicz M., Synthetic hydroxyapatite in pharmaceutical applications, *Ceramics International*, 42, 2472-2487, **2016**.

[6] Hendi A. A., Hydroxyapatite based nanocomposite ceramics, *Journal of Allays and Compounds*, 712, 147-151, **2017**.

[7] Kubasiewicz-Ross P., Hadzik J., Seeliger J., Kozak K., Jurczyszyn K., Gerber H., Dominiak M., Kunert-Keil C., New nano-hydroxyapatite in bone defect regeneration: a histological study in rats, *Annals of Anatomy*, 213, 83-90, **2017**.

[8] Szczes A., Holysz L., Chibowski E., Synthesis of hydroxyapatite for biomedical applications, *Advances in Colloid and Interface Science*, 249, 321-330, **2017**.

[9] Herliansyah M. K., Hamdi M., Ide-Ektessabi A., Wildan M. W., Toque J. A., The influence of sintering temperature on the properties of compacted bovine hydroxyapatite, *Mater Sci Eng C*, 29, 1674-1680, **2009**.

[10] Li B., Zhang K., Yang W., Yin X., Liu Y., Enhanced corrosion resistance of HA/$CaTiO_3$/TiO_2/PLA coated AZ31 alloy, *J Taiwan Inst Chem Eng*, 59, 465-473, **2016**.

[11] Dubey A. K., Mallik P. K., Kundu S., Basu B., Dielectric and electrical conductivity properties of multi-stage spark plasma sintering HA-$CaTiO_3$ composites and comparison with conventionally sintered materials, *J Eur Soc*, 33, 15-16, 3445-3453, **2013**.

[12] Ravikumar K., Mallik P. K., Basu B., Twinning induced enhancement of fracture toughness in ultrafine grained hydroxyapatite-calcium titanate composites, *Journal of the European Ceramic Society*, 36, 805-815, **2016**.

[13] Salma-Ancane K., Stipniece L., Irbe Z., Effect of biogenic and synthetic starting materials on the structure of hydroxyapatite bioceramics, *Ceramics International*, 42, 9504-9510, **2016**.

[14] Oliveira I. R., Andrade T. L., Araujo K. C. M. L., Luz A. P., Pandolfelli V. C., Hydroxyapatite synthesis and the benefits of its blend with calcium alumiinate cement, *Ceramics International*, 42, 2542-2549, **2016**.

[15] Li R., Chen K., Li G., Han G., Yu S., Yao J., Cai Y., Structure design and fabrication of porous hydroxyapatite microspheres for cell delivery, *Journal of Molecular Structure*, 1120, 34-41, **2016**.

[16] Dick T. A., Dos Santos L. A., In situ synthesis and characterization of hydroxyapatite/natural rubber composites for biomedical applications, *Materials Science and Engineering C*, 77, 874-882, **2017**.

[17] Tan C. Y., Yaghoubi A., Ramesh S., Adzila S., Purbolaksono J., Hassan M. A., Kutty M. G., Sintering and mechanical properties of MgO-doped nanocrystalline hydroxyapatite, *Ceram Int*, 39, 8, 8979-8983, **2013**.

[18] Ciobanu C. S., Iconaru S. L., Pasuk I., Vasile B. S., Lupu A. R., Hermenean A., Dinischiotu A., Predoi D,. Structural properties of silver doped hydroxyapatite and their biocompatibility, *Mater Sci Eng C*, 33, 1395-1402, **2013**.

[19] Yu W., Wang X., Zhao J., Tang Q., Wang M., Ning X., Preparation and mechanical properties of reinforced hydroxyapatite bone cement with nano-ZrO2, *Ceram Int*, 41, 9, 10600-10606, **2015**.

[20] Slosarczyk A., Zima A., Paszkiewicz Z., Szczepanak J., De Aza A. H., Chroscicka A., The influence of titanium on physicochemical properties of ti-modified hydroxyapatite materials, *Ceram Mater*, 62, 3, 369-375, **2010**.

[21] Dubey A. K., Basu B., Balani K., Guo R., Bhalla A. S., Multifunctionality of perovskites $BaTiO_3$ and $CaTiO_3$ in a composite with hydroxyapatite as orthopedic implant materials, *Integr Ferroelectr*, 131, 1, 119-126, **2011**.

[22] Khusayfan N. M., Ferroelectric properties of Ce doped hydroxapatite nanoceramics, *Journal of Alloys and Compounds*, 685, 350-354, **2016**.

[23] Sivaperumal V. R., Mani R., Nachiappan M. S., Arumugam K., Direct hydrothermal synthesis of hydroxyapatite/alumina nanocomposite, *Materials Characterization*, 134, 416-421, **2017**.

[24] Lowry N., Han Y., Meenan B. J., Boyd A. R., Strontium and zinc co-substituted nanophase hydroxyapatite, *Ceramics International*, 46, 12070-12078, **2017**.

[25] Barakat A. M. N., Khil M. S., Omran A. M., Sheikh F. A., Kim H. Y., Extraction of pure natural hydroxyapatite from the bovine bones bio waste by three different methods, *J Mater Process Technol*, 209, 8, 3408-3415, **2009**.

[26] Ramírez M. A., Parra R., Reboredo M. M., Varela J. A., Castro M. S., Ramajo L., Elastic modulus and hardness of $CaTiO_3$, $CaCu_3Ti_4O_{12}$ and $CaTiO_3$/$CaCu_3Ti_4O_{12}$ mixture, *Mater Lett*, 64, 10, 1226-1228, **2010**.

[27] Zhuang J., Tian Q., Lin S., Yang W., Chen L., Liu P., Precursor morphology-controlled formation of perovskites $CaTiO_3$ and their photo-activity for As(III) removal, *Appl Catal B*, 156-157, 108-115, **2014**.

[28] Ergun C., Novel machinable calcium phosphate/$CaTiO_3$ composites, *Ceram Int*, 37, 3, 1143-1146, **2011**.

[29] Dong W., Song B., Meng W., Zhao G., Han G., A simple solvothermal process to synthesize $CaTiO_3$ microspheres and its photocatalytic properties, *Appl Surf Sci*, 349, 272-278, **2015**.

[30] Wu S., Tu B., Lin J., Wang Z., Wang X., Shen M., Hu R., Evaluation of the biocompatibility of a hydroxyapatite-$CaTiO_3$ coating in vivo, *Biocybern Biomed Eng*, 35, 4, 296-303, **2015**.

[31] Linh N. T. B., Mondal D., Lee B. T., In vitro study of $CaTiO_3$–hydroxyapatite composites for bone tissue engineering, *J Tissue Eng Biomater*, 60, 6, 722-729, **2014**.

[32] Ozturk S., Yetmez M., Studies on characterzation of bovine hydroxyapatite/$CaTiO_3$ biocomposites, *Adv Mater Sci Eng*, 6987218, 1-7, **2016**.

[33] Dubey A. K., Tripathi G., Basu B., Characterization of hydroxyapatite-perovskite ($CaTiO_3$) composites: phase evaluation and cellular response, *J Biomed Mater Res B Appl Biomater*, 95, 2, 320-329, **2010**.

[34] Yetmez M., Kocer L., Erdogan H., Demirci I., Vibro-acoustic analysis of post-impacted sandwich panels, *Materialwiss Werkstofftech*, 46, 4-5, 440-445, **2015**.
[35] Ozturk S., Numerical and experimental investigation of the effect of sintering temperature on physical and mechanical properties of hydroxyapatite/calcium titanate composites, PhD thesis, Bulent Ecevit University, Turkey, **2017**.
[36] Dahil L., Başpınar S., Karabulut A., Gözenekli Malzemelerin Sönümlemeye Etkisi, *AKU-J. Sci.*, 11, 1–7, **2011**.